



## Stability of emulsion liquid membrane and membrane phase reaction spectrum study of $\text{NH}_3\cdot\text{H}_2\text{O}$ system

Chengzhi Jiang, Xuke Sun\*

School of Environmental and Chemical Engineering, Shenyang Ligong University, Shenyang, China, Tel. +86 13998122505; email: zebra\_jiang1@163.com, Tel. +86 15998192676; email: sylg\_sun2013@163.com

Received 14 January 2015; Accepted 15 September 2015

### ABSTRACT

This paper presents a study on the stability of emulsion liquid membrane (ELM) and membrane phase reaction spectrum in  $\text{NH}_3\cdot\text{H}_2\text{O}$  system. ELM was made up of kerosene, Span 80, tributyl phosphate (TBP), liquid paraffin, and ammonia ( $\text{NH}_3\cdot\text{H}_2\text{O}$ ). Effect of Span 80, TBP and  $\text{NH}_3\cdot\text{H}_2\text{O}$  concentrations, stirring speed and oil phase volume fraction on the emulsion stability were investigated by the conductivity method, respectively. Microscopic photographic technology was used to study emulsion droplets size and distribution. The membrane internal phase reaction was explored with Raman spectra of the primary emulsion and emulsion after extraction. The stable emulsion was obtained at Span 80 concentration of 5–7%, TBP concentration of 3–4%, oil phase volume fraction of 50%, and stirring speed of 4,000–5,000 rpm. A moderate Raman peak was observed for complex  $[\text{Ni}(\text{TBP})_n]^{2+}$  at  $510\text{ cm}^{-1}$ , which indicates occurrence of membrane phase reaction. The reuse of oil phase after demulsification was tested, and its extraction efficiency for  $\text{Ni}^{2+}$  almost kept constant.

*Keywords:* Emulsion liquid membrane; Stability; Conductivity; Raman spectrum; Membrane phase reaction

### 1. Introduction

Emulsion liquid membrane (ELM) is an emerging technique for the separation of contaminants such as metals [1–5], weak acids/bases [6], aniline [7], and hydrocarbons [8], due to its advantages of high surface areas, fast extraction rate, and high efficiency [9]. ELM is a three-phase system consisting of internal, membrane, and external water phases. This process generally includes four steps: emulsion preparation, mixing, separation, and demulsification [10].

Many applications of ELM have been reported in recent years, especially in the aspect of treatment of

wastewaters containing inorganic and organic pollutants. Zhao et al. [11] and Chakraborty et al. [12] reported the removal of chromium ions from aqueous solution with ELM. Organic pollutants, such as alcohol [13], acetaminophen [14], and phenolic compounds [15] had been successfully extracted from aqueous solution using this technology.

The stability and demulsification of emulsion have significant influence on the extraction efficiency of ELM. Chakraborty et al. [16] studied the important variables affecting sauter mean diameter of emulsion droplets, including injection method of emulsion, stirring speed, oil phase viscosity and so on. Li et al. [17] reported that the rapid extraction rate and good stability of emulsion were obtained, when emulsion

\*Corresponding author.

droplets are at the range of 0.3–10  $\mu\text{m}$ . The emulsion including ionic liquid  $[\text{BMIM}]^+[\text{NTf}_2]^-$  presented a good stability during the extraction of ionized nanosilver [18]. Ahmad et al. [19] reported the extraction of  $\text{Cd}^{2+}$  with ELM and found that  $\text{Cd}^{2+}$  reached the highest removal rate, when droplet diameter was the smallest.

The objective of the present work was to investigate the effect of Span 80, TBP and  $\text{NH}_3\cdot\text{H}_2\text{O}$  concentrations, oil phase volume fraction, and stirring speed on the emulsion stability by conductivity method, respectively. The microscopic photographic technology was also used to observe the emulsion droplets size and distribution. Membrane phase reaction was explored with Raman spectra of the primary emulsion and emulsion after extraction of  $\text{Ni}^{2+}$ . Reuse of oil phase after demulsification for the extraction of  $\text{Ni}^{2+}$  was also tested.

## 2. Experimental

### 2.1. Chemicals

Sorbitan monooleate (Span 80), tributyl phosphate (TBP), liquid paraffin,  $\text{NH}_3\cdot\text{H}_2\text{O}$ , nickelous sulfate, and kerosene (commercially available) were used in this experiment. If no special instruction was given, all reagents used were of analytical grade, and were purchased from Sinopharm Chemical Reagent Co., Ltd. All aqueous solutions were prepared with deionized water.

### 2.2. Procedures

According to certain proportion, kerosene (membrane solvent), Span 80 (surfactant agent), TBP (carrier), and liquid paraffin (membrane intensifier) were added into the digital high-speed mixed emulsifying device and the solution was stirred at a certain speed for 5 min, and then internal phase water  $\text{NH}_3\cdot\text{H}_2\text{O}$  at 10 mL/min speed was added into the solution. Then, the mixed solution was stirred continuously at different speeds in the range of 3,000–7,000 rpm for different time. After standing for 5 h, the primary emulsion was poured into external aqueous phase containing the  $\text{Ni}^{2+}$ .

The volume ratio of the primary emulsion to the external aqueous phase was kept at 1:3 [20]. The mixed solution was stirred at 200 rpm speed for 15 min using six combined electric blender. Heating-centrifugal combined demulsification was carried out in the digital thermostatic water bath for 45 min at 90°C, and the centrifugal precipitator for 15 min at the speed of 4,000 rpm, respectively. The obtained oil

phase after demulsification was reused to extract the nickel ions according to the previous procedure.

### 2.3. Characterization and analysis

The emulsion stability was characterized by conductivity method [21] and microscopic photographic technology [22], respectively. Conductivity of emulsion was measured with conductivity meter (DDS-11A, Zhejiang, China). Generally, the lower the conductivity is, the more stable the emulsion is. Emulsion droplet morphology was observed with color image microscopy (59XC-MC, Beijing, China). After extraction and separation, concentration of the nickel ion of external aqueous phase was determined by measuring the absorbance at 530 nm wavelength with vis spectrophotometer (721, Shanghai, China). Raman spectra of the primary oil phase, primary emulsion, emulsion after extraction and separation, and oil phase after demulsification were recorded with UV high temperature Raman spectrograph (HR800, Paris, France) [23–26], respectively. Membrane phase reaction was explored by comparing Raman spectra of the primary emulsion with emulsion after extraction and separation. For comparison, Raman spectra of TBP and TBP +  $\text{Ni}^{2+}$  systems were also recorded.

## 3. Results and discussion

### 3.1. Stability of emulsion

Effect of Span 80, TBP, and  $\text{NH}_3\cdot\text{H}_2\text{O}$  concentrations, oil phase volume fraction, stirring speed, and stirring time were investigated on the emulsion stability of  $\text{NH}_3\cdot\text{H}_2\text{O}$  system.

#### 3.1.1. Effect of Span 80 concentration on emulsion stability

The effect of Span 80 concentration on conductivity of  $\text{NH}_3\cdot\text{H}_2\text{O}$  system is shown in Fig. 1.

It can be seen from the results that Span 80 concentration has a significant effect on conductivity of the emulsion. When Span 80 concentration was increased from 3 to 5%, conductivity of the emulsion decreased gradually; when Span 80 concentration was at the range of 5–7%, conductivity of the emulsion nearly remained unchanged; when Span 80 concentration was increased from 7 to 10%, the conductivity of the emulsion increased. These results indicate that when Span 80 concentration is at the range of 5–7%, the emulsion is more stable, and lower (below 5%) or higher (above 7%) concentration is not favorable for

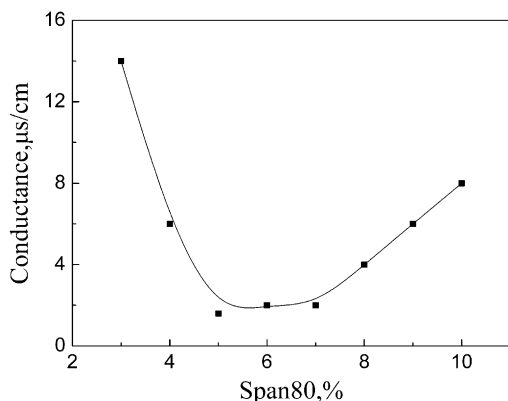


Fig. 1. Effect of Span 80 concentration on conductivity of  $\text{NH}_3\cdot\text{H}_2\text{O}$  system.

the emulsion stability. The reasons for the results can be explained as follows.

As a polymeric surfactant, molecular weight of Span 80 is high and its hydrophobic hydrocarbon chain is long, so that the adsorption membrane layer of oil-water interface becomes much thicker with slightly increasing Span 80 concentration. Simultaneously, viscosity of the emulsion and probability of the chain entanglement are also increased with increasing Span 80 concentration. Increase in the viscosity will inhibit the settlement of droplets and favor the formation of small droplets and their uniform distribution. The interfacial membrane becomes more compact and intensive with increasing Span 80 concentration, which makes the emulsion become more stable.

However, if Span 80 concentration is further increased, area of the phase interface and the surface free energy will increase, which is unfavorable for emulsion stability.

### 3.1.2. Effect of TBP concentration on emulsion stability

The effect of TBP concentration on conductivity of  $\text{NH}_3\cdot\text{H}_2\text{O}$  system is given in Fig. 2.

It can be seen from the results that conductivity of the emulsion decreased, when TBP concentration increased from 2 to 3%. At the range of 3–4%, conductivity of the emulsion was almost constant. When TBP concentration was further increased from 4 to 8%, continuous increase in conductivity was observed. The results show that when TBP concentration is at the range of 3–4%, the emulsion is more stable and lower (below 3%) or higher (above 4%) concentration is not favorable for the emulsion stability. With increase in TBP concentration, the viscosity of the emulsion is also increased, which is favorable for the stability of the

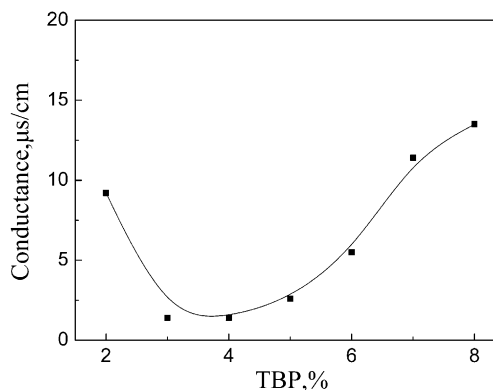


Fig. 2. Effect of TBP concentration on conductivity of  $\text{NH}_3\cdot\text{H}_2\text{O}$  system.

emulsion. On the other hand, excessive carriers not only increase the viscosity of liquid membrane but also compete with the surfactant for the interface space, leading to the decrease in the interface space occupied by Span 80. Consequently, the further increase in TBP concentration after 4% decreases the emulsion stability.

### 3.1.3. Effect of $\text{NH}_3\cdot\text{H}_2\text{O}$ concentration on emulsion stability

The effect of  $\text{NH}_3\cdot\text{H}_2\text{O}$  concentration in internal phase on conductivity of emulsion is shown in Fig. 3.

Different from the Span 80 and TBP,  $\text{NH}_3\cdot\text{H}_2\text{O}$  concentration has little influence on conductivity of emulsion. When  $\text{NH}_3\cdot\text{H}_2\text{O}$  concentration was increased from 0.5 to 1.0 mol/L, the conductivity of emulsion significantly decreased. When  $\text{NH}_3\cdot\text{H}_2\text{O}$  concentration was at the range of 1.0–2.0 mol/L, the conductivity of

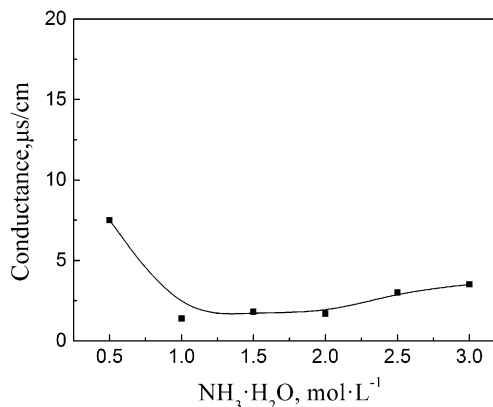


Fig. 3. Effect of  $\text{NH}_3\cdot\text{H}_2\text{O}$  concentration in internal phase on conductivity of emulsion.

emulsion was almost constant. When  $\text{NH}_3\cdot\text{H}_2\text{O}$  concentration was further increased, the conductivity of emulsion slightly increased. A possible reason for such behavior may be related to the adsorption of  $\text{NH}_4^+$  onto membrane phase interface and hydrolysis of Span 80. The adsorption of  $\text{NH}_4^+$  may change the double layer structure on the membrane phase interface and increases the electrostatic repulsion among the droplets and consequently facilitate stability of the emulsion. On the other hand, hydrolysis of Span 80 occurs under alkali conditions, which may decrease the stability of the emulsion. When  $\text{NH}_3\cdot\text{H}_2\text{O}$  concentration is at the range of 0.5–1.0 mol/L, increase in the electrostatic repulsion with increasing  $\text{NH}_3\cdot\text{H}_2\text{O}$  concentration may be predominant, while at the range of 2.0–3.0 mol/L, the hydrolysis of Span 80 may play a more important role with respect to the emulsion stability. At the range of 1.0–2.0 mol/L, the effect of these two factors on the stability of emulsion may be equivalent.

#### 3.1.4. Effect of oil phase volume fraction on emulsion stability

Effect of oil phase volume fraction on conductivity of  $\text{NH}_3\cdot\text{H}_2\text{O}$  system is given in Fig. 4.

It can be seen from the results that when oil phase volume fraction was increased from 20 to 50%, conductivity of the emulsion decreased continuously. After that, conductivity of the emulsion increased with increasing the oil phase volume fraction. This means that the emulsion is the most stable at the oil phase volume fraction of 50%.

Increase in the oil phase volume fraction makes the membrane layer to thicken, and the emulsion becomes more stable. However, when the oil phase volume fraction exceeds 50%, the emulsion stability becomes poor. Although the emulsion type (W/O or

O/W) is related to the surfactant species, the two emulsion types with different proportion may co-exist in a liquid membrane system [27]. At a higher oil phase volume fraction, the proportion of O/W type may be increased and becomes the predominant one, which is unfavorable for the emulsion stability.

#### 3.1.5. Effect of stirring speed on emulsion stability

In the emulsion preparation stage, internal water phase is dispersed into the membrane phase by the stirring. In general, stirring speeds higher than 2,000 rpm are used to prepare the emulsion in the experiment [11]. In the present work, stirring speeds at the range of 3,000–7,000 rpm were used to prepare the emulsion. The effect of stirring speed on conductivity of  $\text{NH}_3\cdot\text{H}_2\text{O}$  system is shown in Fig. 5.

The conductivity of emulsion was higher at the speed of 3,000 rpm, due to the fact that the size and distribution of emulsion droplets is not uniform at that speed [28]. When stirring speed was increased to 4,000–5,000 rpm, the conductivity of emulsion was lower compared with that at 3,000 rpm. This is due to the fact that small emulsion droplets of uniform of distribution were obtained at the speed of 4,000–5,000 rpm. That shows that the dispersibility of the droplets is better. When stirring speed was further increased, the conductivity was also increased. The reason may be that too high stirring speed is easy to make the emulsion droplets appear coalescence and destroy the uniform distribution of the droplets.

#### 3.1.6. Effect of stirring time on emulsion droplet size and distribution

Appropriate stirring time is beneficial to the uniform distribution of surfactant and carrier in membrane phase, which further enhances the emulsion

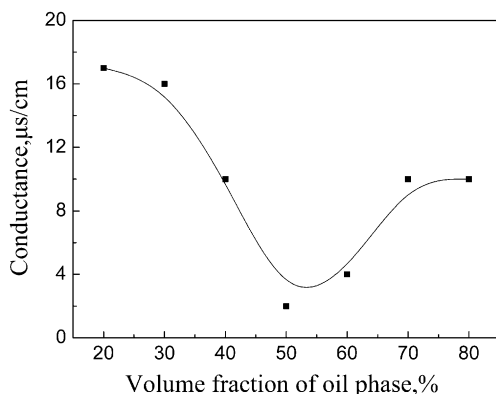


Fig. 4. Effect of oil phase volume fraction on conductivity of  $\text{NH}_3\cdot\text{H}_2\text{O}$  system.

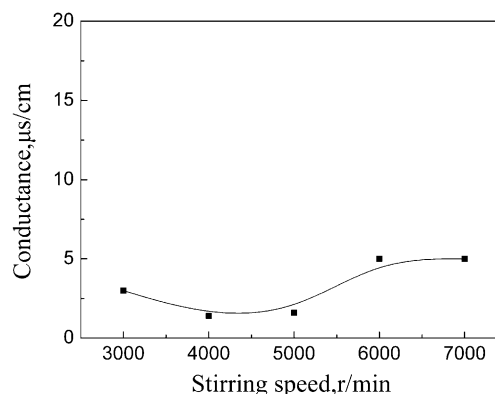


Fig. 5. Effect of stirring speed on conductivity of  $\text{NH}_3\cdot\text{H}_2\text{O}$  system.

stability. Small emulsion droplets and their uniform distribution result in the formation of stable emulsion. The size and distribution of emulsion droplets are related to stirring speed and stirring time. In order to investigate the effect of stirring time on the size and distribution of emulsion droplets, the morphology of emulsion droplets at different stirring time (stirring speed kept at 4,000 rpm) was observed by the microscopic photographic technology and the results are given in Fig. 6(a)–(h).

It can be seen that in the test range of 5–40 min, the stirring time had an influence on the size and distribution of the emulsion droplets. The emulsion droplets were relatively large and their distribution was not uniform at 5–10 min; when the stirring time was kept at 15–25 min, emulsion droplets were small and their distribution was relatively uniform. However, when the stirring time was further increased, coalescence of the emulsion droplets appeared. The reason for the effect of stirring time on the size and

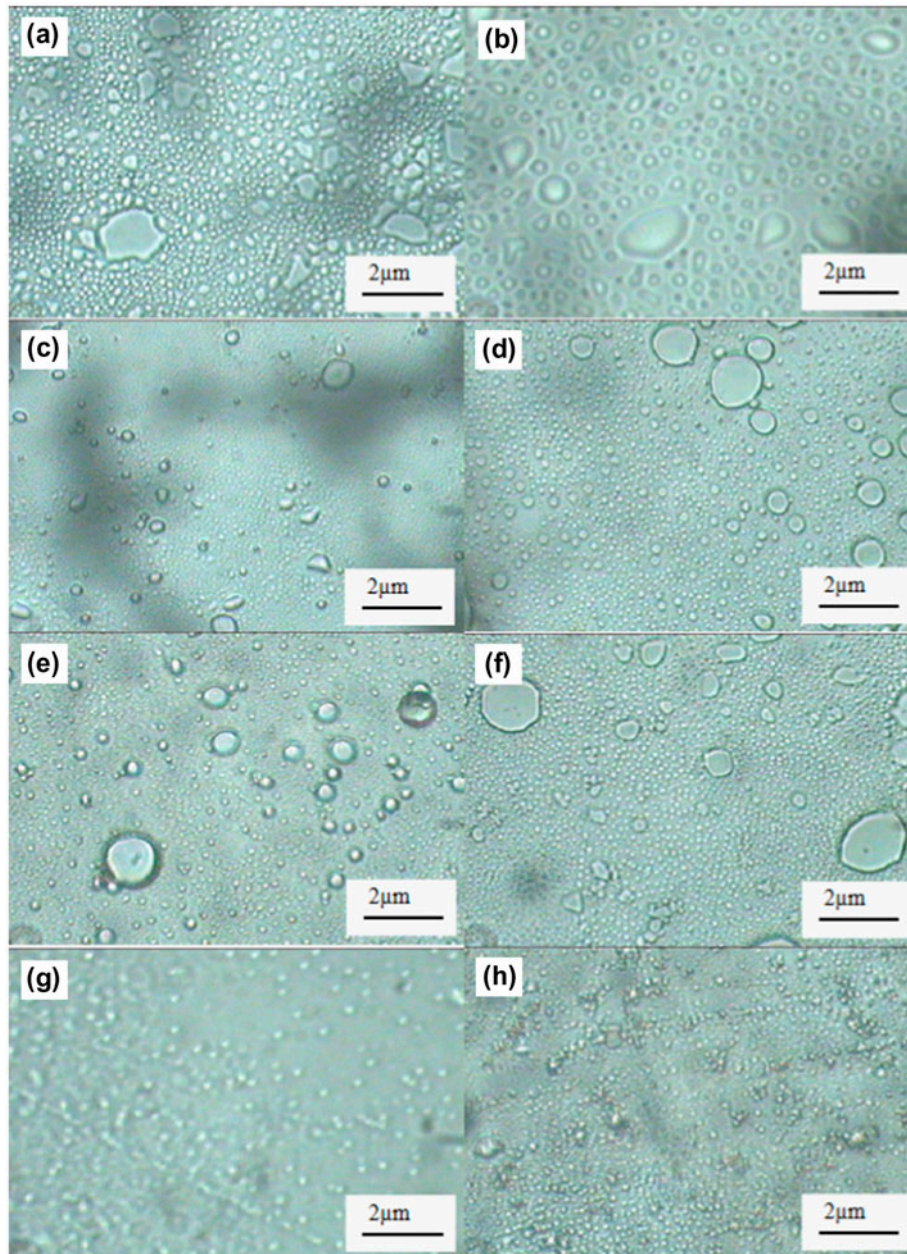


Fig. 6. Effect of stirring time on emulsion droplets size and distribution of  $\text{NH}_3\text{-H}_2\text{O}$  system: (a) 5 min, (b) 10 min, (c) 15 min, (d) 20 min, (e) 25 min, (f) 30 min, (g) 35 min, and (h) 40 min.

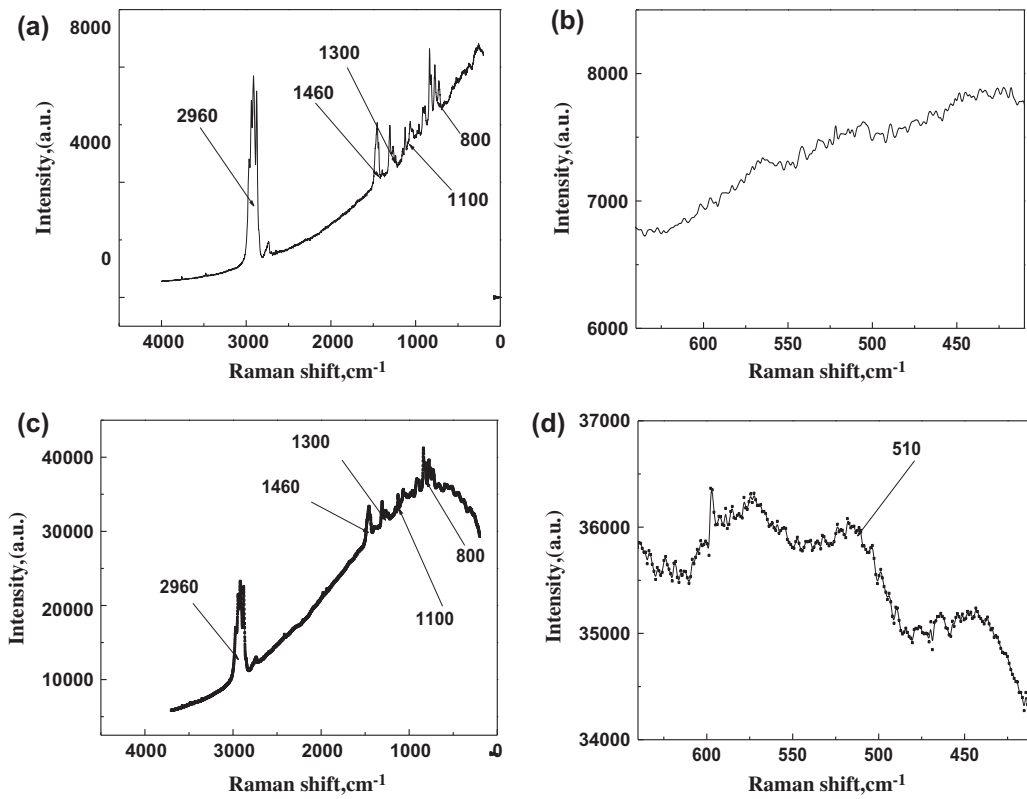


Fig. 7. Raman spectra of TBP and TBP + Ni<sup>2+</sup>: (a) TBP, (b) enlarged drawing of (a), (c) TBP + Ni<sup>2+</sup>, and (d) enlarged drawing of (c).

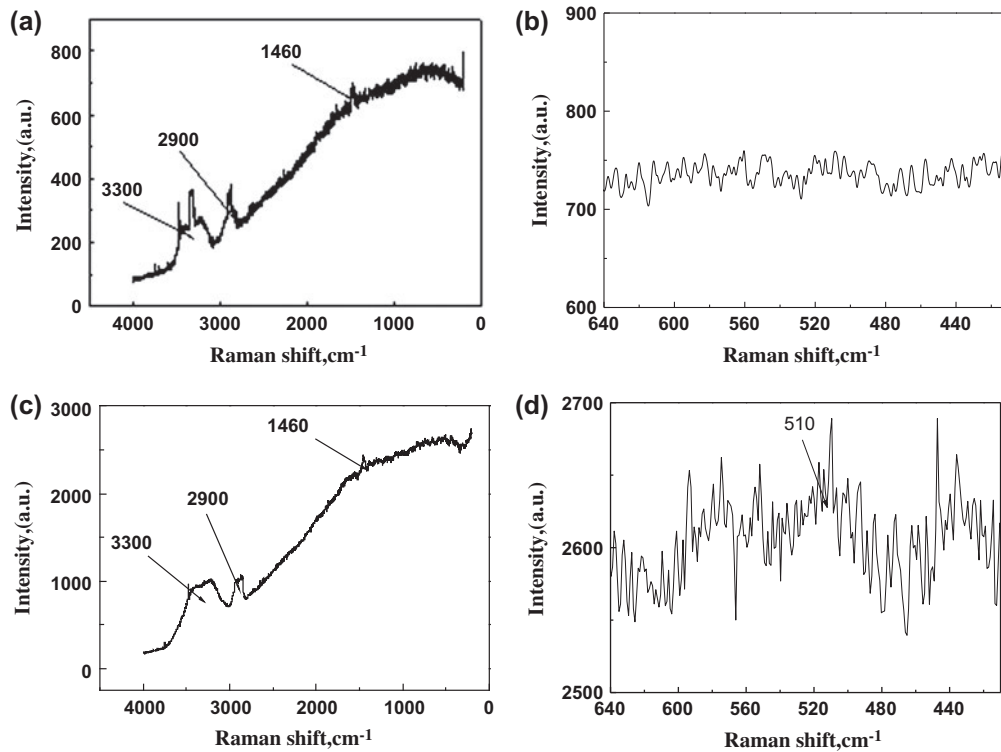


Fig. 8. Raman spectra of the primary emulsion and emulsion after extraction: (a) the primary emulsion, (b) enlarged drawing of (a), (c) emulsion after extraction, and (d) enlarged drawing of (b).

distribution of emulsion droplets is similar to that for the effect of stirring speed on the emulsion stability.

### 3.2. Raman spectra of different systems

In order to investigate the membrane phase reaction of extract  $\text{Ni}^{2+}$  in  $\text{NH}_3\cdot\text{H}_2\text{O}$  system, Raman spectra were determined for different systems.

#### 3.2.1. Raman spectra of TBP and TBP + $\text{Ni}^{2+}$

Raman spectra of TBP and TBP +  $\text{Ni}^{2+}$  are shown in Fig. 7(a) and (c). It can be seen that there was an intensive absorption peak at  $2,960\text{ cm}^{-1}$ , which was attributed to the stretching vibration of  $-\text{CH}_3$ . Peaks at  $1,460$  and  $1,300\text{ cm}^{-1}$  in Fig. 7(a) and (c) corresponded to bending vibration of  $-\text{CH}_2$  and angular vibration of  $-(\text{CH}_2)_3$ , respectively. Several absorption peaks in the region  $1,100\text{--}800\text{ cm}^{-1}$  corresponded to the characteristic Raman spectrum bands of C–H [29].

The enlarged drawing of Raman spectra of TBP and TBP +  $\text{Ni}^{2+}$  between  $410$  and  $640\text{ cm}^{-1}$  are shown in Fig. 7(b) and (d). There was a Raman peak around  $510\text{ cm}^{-1}$  (Fig. 7(d)), corresponding to the vibration of  $\text{O}=\text{P}-\text{O}$ , which indicated the formation of complex molecule between TBP and  $\text{Ni}^{2+}$  [30].

#### 3.2.2. Raman spectra of the primary emulsion and emulsion after extraction

Raman spectra of the primary emulsion and emulsion after extraction are also recorded and shown in Fig. 8(a) and (c). Apart from the peaks at  $1,460$  and  $2,960\text{ cm}^{-1}$ , a peak at  $3,300\text{ cm}^{-1}$  in Fig. 8(a) and (c) was observed, which corresponded to the stretching vibration of  $\text{NH}_3^+$ . The enlarged drawing of Raman spectra of the primary emulsion and emulsion after extraction between  $410$  and  $640\text{ cm}^{-1}$  are shown in Fig. 8(b) and (d). A peak at  $510\text{ cm}^{-1}$  for the emulsion after extraction appeared (Fig. 8(d)). This result indicates the formation of complex  $[\text{Ni}(\text{TBP})_n]^{2+}$  and occurrence of membrane phase reaction.

#### 3.2.3. Raman spectra of the primary oil phase and oil phase after demulsification

Raman spectra of the primary oil phase and oil phase after demulsification for the  $\text{NH}_3\cdot\text{H}_2\text{O}$  system are given in Fig. 9(a) and (b), respectively. Peaks at  $2,900$ ,  $1,460$ , and  $1,300\text{ cm}^{-1}$  are all observed in Fig. 9(a) and (b), which corresponded to the stretching vibration of  $-\text{CH}_3$ , bending vibration of  $-\text{CH}_2$ , and angular vibration of  $-(\text{CH}_2)_3$ , respectively. Several

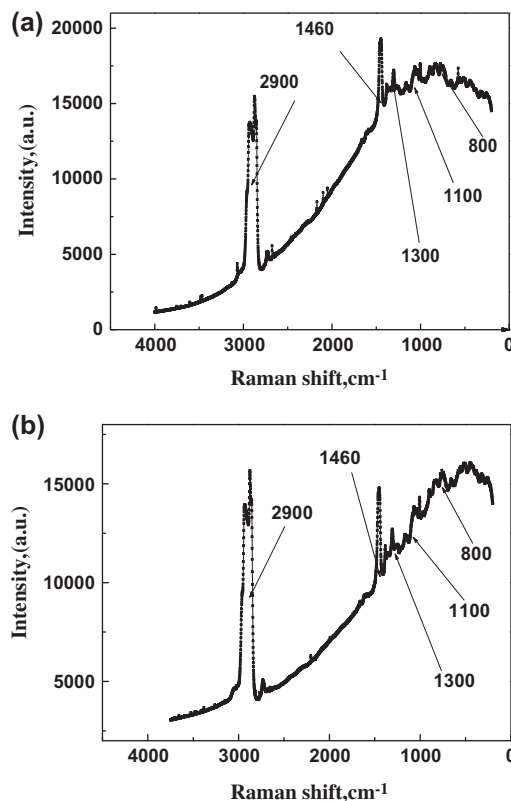


Fig. 9. Raman spectra of the primary oil phase and oil phase after demulsification: (a) the primary oil phase and (b) oil phase after demulsification.

weak absorption peaks in the range between  $800$  and  $1,100\text{ cm}^{-1}$  belonged to the characteristic Raman spectrum band of C–H in two Raman spectra. Comparing the Raman spectrum of the primary oil phase with that of oil phase after demulsification shown in Fig. 9(a) and (b), it can be found that there is almost no difference in the Raman spectra for the two systems. The results show that the chemical bonds of various components in the oil phase have not been destroyed in the physical demulsification process, and that the oil phase after demulsification may be reused.

### 3.3. Reuse of oil phase

The oil phase after demulsification was reused to prepare the emulsion according to the procedure

Table 1  
The relationship between reuse times and extraction efficiency of  $\text{Ni}^{2+}$

Reuse times	0	1	2	3
Extraction efficiency of $\text{Ni}^{2+}$ (%)	92	90	90	90

mentioned above. The extraction efficiency of  $\text{Ni}^{2+}$  for the different reuse times of the oil phase after demulsification is given in Table 1. It can be seen from the results that in the test range, the reuse times has little influence on the extraction efficiency of  $\text{Ni}^{2+}$ . After three times of emulsification and demulsification, the extraction efficiency is still up to 90%, which is close to that obtained with the fresh oil phase (92%). The high stability of the oil phase in the reused process for the extraction of  $\text{Ni}^{2+}$  with ELM is of environmental and economic interest.

#### 4. Conclusions

Stability of ELM, reaction of membrane phase with  $\text{Ni}^{2+}$  in  $\text{NH}_3\text{-H}_2\text{O}$  systems and reuse of oil phase were investigated. The following conclusions can be withdrawn from the results: The emulsion stability is related to some factors such as Span 80, TBP concentrations and oil phase volume fraction. The stable emulsion is obtained at Span 80 concentration of 5–7%, TBP concentration of 3–4%, and oil phase volume fraction of 50%.  $\text{NH}_3\text{-H}_2\text{O}$  concentration, stirring speed, and stirring time have relatively little influence on the emulsion stability. Based on the Raman spectra of the primary emulsion and emulsion after extraction, the membrane phase reaction is proved in  $\text{NH}_3\text{-H}_2\text{O}$  system. The oil phase after demulsification can be effectively reused for the extraction of  $\text{Ni}^{2+}$  with ELM. The high stability of the oil phase in the reused process is of environmental and economic interest.

#### Acknowledgments

We gratefully acknowledge the financial support by the Education Department of Liaoning province (L2013088), the fund project of Public welfare scientific research of Science and Technology Department of Liaoning province (2013003010), and the open fund of Key Laboratory of wastewater treatment technology of Shenyang Ligong University.

#### References

- [1] F. Valenzuela, C. Fonseca, C. Basualto, O. Correa, C. Tapia, J. Sapag, Removal of copper ions from a waste mine water by a liquid emulsion membrane method, *Miner. Eng.* 18 (2005) 33–40.
- [2] S. Bourenane, M. Samar, A. Abbaci, Extraction of cobalt and lead from waste water using a liquid surfactant membrane emulsion, *Acta Chim. Solv.* 50 (2003) 663–675.
- [3] R.A. Kumbasar, Separation and concentration of cobalt from zinc plant acidic thiocyanate leach solution containing cobalt and nickel by an emulsion liquid membrane using triisooctylamine as carrier, *J. Hazard. Mater.* 333 (2009) 118–124.
- [4] R.A. Kumbasar, Extraction of chromium (VI) from multicomponent acidic solutions by emulsion liquid membranes using TOPO as extractant, *J. Hazard. Mater.* 167 (2009) 1141–1147.
- [5] M.S. Gasser, N.E. El-Hefny, J.A. Daoud, Extraction of Co(II) from aqueous solution using emulsion liquid membrane, *J. Hazard. Mater.* 151 (2008) 610–615.
- [6] C. Wang, A.L. Bunge, Multisolute extraction of organic acids by emulsion liquid membranes. I. Batch experiments and models, *J. Membr. Sci.* 53 (1990) 71–103.
- [7] R. Devulapalli, F. Jones, Separation of aniline from aqueous solutions using emulsion liquid membranes, *J. Hazard. Mater.* 70 (1999) 157–170.
- [8] M.T.A. Reis, O.M.F. de Freitas, L.M. Ferreira, J.M.R. Carvalho, Extraction of 2-(4-hydroxyphenyl)ethanol from aqueous solution by emulsion liquid membranes, *J. Membr. Sci.* 269 (2006) 161–170.
- [9] A.L. Ahmad, A. Kusumastuti, C.J.C. Derek, B.S. Ooi, Emulsion liquid membrane for heavy metal removal: An overview on emulsion stabilization and destabilization, *Chem. Eng. J.* 171 (2011) 870–882.
- [10] A. Hachemaoui, K. Belhamei, H.J. Bart, Emulsion liquid membrane extraction of Ni(II) and Co(II) from acidic chloride solutions using bis-(2-ethylhexyl) phosphoric acid as extractant, *J. Coord. Chem.* 63 (2010) 2337–2348.
- [11] L. Zhao, D. Fei, Y. Dang, X. Zhou, J. Xiao, Studies on the extraction of chromium(III) by emulsion liquid membrane, *J. Hazard. Mater.* 178 (2010) 130–135.
- [12] S. Chakraborty, S. Datta, P. Bhattacharya, Studies on extraction of chromium(VI) from acidic solution by emulsion liquid membrane, *Indian J. Chem. Technol.* 12 (2005) 713–718.
- [13] B.S. Chanukya, N.K. Rastogi, Extraction of alcohol from wine and color extracts using liquid emulsion membrane, *Sep. Purif. Technol.* 105 (2013) 41–47.
- [14] S. Chaouchi, O. Hamdaoui, Acetaminophen extraction by emulsion liquid membrane using Aliquat 336 as extractant, *Sep. Purif. Technol.* 129 (2014) 32–40.
- [15] A. Balasubramanian, S. Venkatesan, Removal of phenolic compounds from aqueous solutions by emulsion liquid membrane containing Ionic Liquid  $[\text{BMIM}]^+[\text{PF}_6]^-$  in Tributyl phosphate, *Desalination* 289 (2012) 27–34.
- [16] M. Chakraborty, C. Bhattacharya, S. Datta, Effect of drop size distribution on mass transfer analysis of the extraction of nickel(II) by emulsion liquid membrane, *Colloids Surf., A: Physicochem. Eng. Aspects* 224 (2003) 65–74.
- [17] N. Li, R.P. Cahn, D. Naden, R.W.M. Lai, Liquid membrane processes for copper extraction, *Hydrometallurgy* 9 (1983) 277–305.
- [18] R.N.R. Sulaiman, N. Othman, N.A.S. Amin, Emulsion liquid membrane stability in the extraction of ionized nanosilver from wash water, *J. Ind. Eng. Chem.* 20 (2014) 3243–3250.
- [19] A.L. Ahmad, A. Kusumastuti, C.J.C. Derek, B.S. Ooi, Emulsion liquid membrane for cadmium removal: Studies on emulsion diameter and stability, *Desalination* 287 (2012) 30–34.

- [20] C. Jiang, X. Zhai, T. Zhang, Extraction nickel from the leaching liquid of laterite ore by emulsion liquid membrane, *Chin. J. Process Eng.* 4 (2010) 691–695.
- [21] K.M. Waszkielis, I. Białobrzewski, K.W. Nowak, Ł. Dzadz, J. Dach, Determination of the thermal conductivity of composted material, *Measurement* 58 (2014) 441–447.
- [22] M.S. Loghdey, S. Varma, S.M. Rajpara, H. Al-Rawi, G. Perks, W. Perkins, Mohs micrographic surgery for dermatofibrosarcoma protuberans (DFSP): A single-centre series of 76 patients treated by frozen-section Mohs micrographic surgery with a review of the literature, *J. Plast. Reconstr. Aesthet. Surg.* 67 (2014) 1315–1321.
- [23] M.S. Refat, K.M. Elsabay, Infrared spectra, Raman laser, XRD, DSC/TGA and SEM investigations on the preparations of selenium metal,  $\text{Sb}_2\text{O}_3$ ,  $\text{Ga}_2\text{O}_3$ ,  $\text{SnO}$  and  $\text{HgO}$  oxides and lead carbonate with pure grade using acetamide precursors, *Bull. Mater. Sci.* 34 (2011) 873–881.
- [24] J.S. Singh, FT-IR and Raman spectra, *ab initio* and density functional computations of the vibrational spectra, molecular geometries and atomic charges of uracil and 5-methyluracil (thymine) *Spectrochim. Acta Part A: Mol. Biomol. Spectrosc.* 137 (2015) 625–640.
- [25] M. Kumru, V. Küçük, M. Kocademir, H.M. Alfanda, A. Altun, L. Sarı, Experimental and theoretical studies on IR, Raman, and UV–Vis spectra of quinoline-7-carboxaldehyde, *Spectrochim. Acta Part A: Mol. Biomol. Spectrosc.* 134 (2015) 81–89.
- [26] V.L. Furer, A.E. Vandyukov, J.P. Majoral, A.M. Caminade, S. Gottis, R. Laurent, V.I. Kovalenko, DFT study of structure, IR and Raman spectra of phosphorus-containing dendron with azide functional group, *Vib. Spectrosc.* 75 (2014) 1–10.
- [27] P. Becher, *Emulsions: Theory and Practice*, Reinhold Publishing Corporation, America, 1957.
- [28] R. Sabry, A. Hafez, M. Khedr, A. El-Hassanin, Removal of lead by an emulsion liquid membrane: Part I, *Desalination* 212 (2007) 165–175.
- [29] Z. Zhu, R. Gu, T. Lu, *Application of Raman Spectrum in Chemistry*, Northeastern University Press, China, 1998.
- [30] A. Ma, X. Cui, L. Tian, Vibration spectrum research of Butyl phosphonic acid monobutyl ester rare earth complex, *J. Henan Univ. (Nat. Sci.)* 36 (2006) 47–50.